1. Samer S. Wahdain[1], 2. A. I. Mohamed[1], 3. Mohd Herwan Sulaiman[1], 4. Mohd Razali Daud[1], 5. Raja Mohd Taufika Raja Ismail[1]

University Malaysia Pahang (1)

ORCID: 1. 0000-0003-1217-6292; 2. 0000-0001-9363-4026; 3. 0000-0003-2590-3807; 5. 0000-0002-2146-1450

Analysis of electric field behaviour for wind turbine blades under the influence of various gas

Abstract. Wind turbines are one of the most important natural sources of energy. The components of atmosphere gases in the surrounding wind turbines that are installed may significantly affect the increasing of electrical field resulting from lighting strikes. Here, we use the initiation and spread of electrical field in various gases O_2, N_2, Ar, Ne and SO_2 to examine the behaviour of electrical field on blade. This study uses the Finite Element Method to investigate the influence of gases on the lightning strike carbon fibre wind turbine blade. We use 3D modelling geometry i n this study to get accurate results for all sides of the blade. The generation of an impulse wave uses three stages with time varying from 0 to 60 μs. It was observed that N_2 and Air give the same reading because Nitrogen represents 72% of the air contents. Thus, our study elucidates that applying various gases can affect the electric field strength.

Streszczenie. Turbiny wiatrowe są jednym z najważniejszych naturalnych źródeł energii. Składniki gazów atmosferycznych w otaczających turbinach wiatrowych, które są zainstalowane, mogą znacząco wpłynąć na zwiększenie pola elektrycznego w wyniku uderzeń pioruna. Tutaj wykorzystujemy inicjację i rozprzestrzenianie się pola elektrycznego w różnych gazach O_2, N_2, Ar, Ne i SO_2, aby zbadać zachowanie pola elektrycznego na ostrzu. Niniejsze badanie wykorzystuje metodę elementów skończonych do zbadania wpływu gazów na uderzenie pioruna łopaty turbiny wiatrowej z włókna węglowego. W tym badaniu używamy geometrii modelowania 3D, aby uzyskać dokładne wyniki dla wszystkich stron łopaty. Generowanie fali impulsowej składa się z trzech etapów w czasie od 0 do 60 μs. Zaobserwowano, że N_2 i powietrze dają ten sam odczyt, ponieważ azot stanowi 72% zawartości powietrza. W ten sposób nasze badanie wyjaśnia, że stosowanie różnych gazów może wpływać na natężenie pola elektrycznego. (Analiza zachowania pola elektrycznego łopat turbiny wiatrowej pod wpływem różnych gazów)

Keywords: lightning protection, Electric field, wind turbine blade
Słowa kluczowe: ochrona odgromowa, pole elektryczne, łopata turbiny wiatrowej.

Introduction

With the development or renewable energy, wind energy systems are quickly developed, responding to the increasing demand for other energy sources [1]. Wind turbines differ from conventional electricity structures by being situated in windy areas and having tall construction averages of over 100 meters [2], [3]. Therefore, wind turbines are particularly vulnerable to lightning strikes due to their exposed location, height, and complex terrain. Lightning is one of the leading causes of catastrophic wind turbine damage, causing millions of dollars in losses each year. For example, a central wind farm in the North Sea in Helgoland (Germany) suffered such enormous losses due to lightning strikes about 15 years ago that its operation was no longer economically efficient [4]. In addition, Multimegawatt wind turbines are tall constructions which is more likely to be struck by regular cloud-to-ground lightning than their surroundings [5].

A lightning protection system is necessary for wind turbines. Lightning damage to wind turbines has become a big issue for manufacturers. The offshore plants now being built will be even more vulnerable to lightning strikes [6], [7].

Lightning on the earth is a complex natural phenomenon bridging two to three miles lengths, time, and energy scales [8]–[10].

Lightning protection tests for large-scale wind turbine blades require high cost, and a limited number and scales are available in the laboratory. However, assuming that the blades are the most vulnerable to damage due to lightning strikes, understand downward streamers phenomena by researching the electric field activity during a thunderstorm[11]–[14].

Most of the previous research focused on the direct effect of lightning strikes on wind turbine blades at different angles of the blades. On the other hand, there is a lack of understanding of the behaviour of lightning strikes concerning time on wind turbines.

As lightning is governed by electrical field, it is important to understand electrical field behaviour on the wind turbine blades. In this study, electrical field distribution on the blade under different gases O_2, N_2, Ar, Ne and SO_2.

This paper focuses on analyzing in the time-dependent study, the electric field distribution under impulse voltage with the various gas that may influence it in 3D and 2D modelling using the Finite Element Method (FEM).

Methodology

FEM is to get approximative solutions to boundary value issues of partial differential equations and mathematics. Numerical approximation and discretization are its main concepts. The variational method reduces the error function to its lowest value and generates a stable solution. It also views the solution domain as consisting of numerous small, connected subdomains called finite elements, assumes a suitable approximation for each element, and then determines the overall satisfying conditions for solving this domain to arrive at the problem's solution [11], [13]–[15].

Modelling Geometry
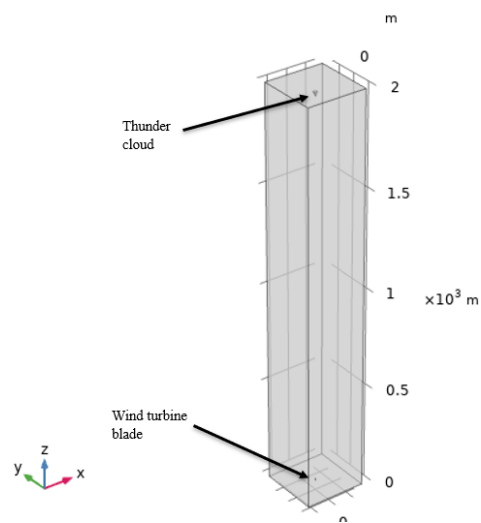
Fig.1. 3D geometry for the whole domain

Throughout the modelling, we use three- and two-dimensional geometry designs. Fig. 1 shows the whole project model; the dimension has been decided to be 300×300×2000 (m). The height of a thundercloud is 2 km from the wind turbine blade [11].

This dimension of cuboid was used around the wind turbine, which was air for modelling the wind turbine environment, and the cone of the top cuboid was used to simulate the background of a thundercloud, as shown in Fig.2 (a).
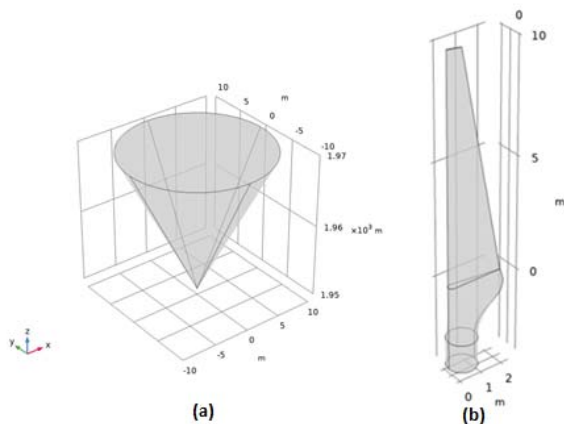
Fig. 2. Geometry design (a) Terminal cone, (b) Wind turbine blade

In Fig.2 (b), the dimension of the wind turbine blade is 2×1×10 m, and the material property of the blade was specified as carbon fibre [16], [17]. Finally, the blade design in Fig. 2 (b) was imported from the CAD.

Domain Gases Properties

To combine the type of gas in this project model, we need to create another domain inside this cuboid in Fig. 1. The total environment is five inside the cuboid, which is five different materials(gas) inside this project model.
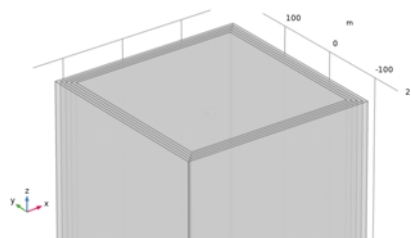
Fig. 3. Gases Domain

Table 1. The properties of each gas layer.

Layer No.	Gas	Properties
1	N_2	78% of the earth's atmosphere has a strong triple bond between its atoms, which is difficult to break apart.
2	O_2	21% of the earth's atmosphere forms two chemical molecules.
3	Ar	1% of earth's atmosphere, produced by potassium breakdown in the earth, inert gas [18]
4	Ne	0.0018% of the earth's atmosphere is created from the air [18],
5	SO_2	Release to the atmosphere by natural sources, particle pollution, are pollutants that contribute to the development of acid rain [19].

The first outer layer inside this cuboid uses air or N_2 then the second layer is O_2, the third layer is **Ar**, the fourth layer is Ne, and lastly, we are using SO_2 to investigate the effect of electric field behaviour on the wind turbine blade

with a different type of gas in the air. Fig. 3 shows the combination of five domains in one model. This method is used to combine the various gases in the whole model of the project. Table 1 defines the properties of each gas layer.

Impulse voltage

Using integrated Function in modelling software, data was imported from SPICE software that was used to model a three-stage impulse generator.
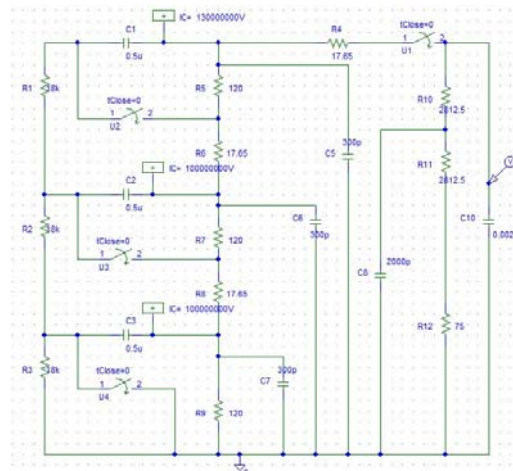
Fig. 4. Impulse generator circuit

Fig. 4 depicts the simulated generator's design. Again, switches were used to approximate the stage sphere gaps, as indicated. Furthermore, several capacitors are charged in parallel in the multi-stage impulse generator.

Fig. 5 shows the maximum impulse voltage is 298.14MV. With a peak voltage of 298.14MV, the time to peak is 1.22 µs. This simulation circuit's peak voltage is lower than required, but we can use this result even though the peak of impulse voltage does not look accurate to achieve 300MV. The tail of the wave (T2), which corresponded to half of the peak voltage, lasted around 40 µs.
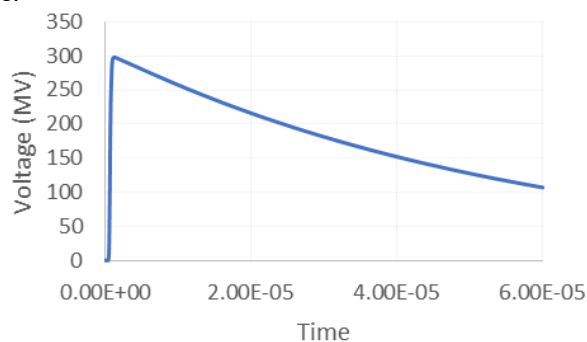
Fig. 5. Impulse output waveform

Numerical analysis

The "electrostatic" under the condition of clearly characterizing the charge distribution calculated the electric field distribution, electric displacement field distribution, and electric potential distribution in dielectrics [11].

The terminal of electric potential is applied to the thunder cloud by selecting all the boundaries of the cone in this model. In addition, the boundary of the turbine blade has been established for the ground terminal. This project analyses by applying impulse voltage to get a better result based on actual lightning events.

The static equation of the electrostatic field is expressed by (1) and (2):

$$(1) \quad \nabla \cdot D = \rho v$$
$$(2) \quad E = -\nabla V$$

The charge conservation equations are represented by (2) and (3), and the zero charges are represented by equation (4):

$$(3) \quad \nabla \cdot (\varepsilon_0 \varepsilon r E) = \rho v$$
$$(4) \quad n \cdot D = 0$$

Where electric displacement vector $\nabla \cdot (\varepsilon_0 \varepsilon r E)$, ε_o is vacuum permittivity, ε_r is the material's relative permittivity.

The Time-Dependent study and study step is used when field variables change over time by using a Time-Dependent Solver to compute the solution over time for a time-dependent or transient simulation. First, select a Time/parameter list method.

This option only appears if active least-squares objective functions are defined in the model. There is two range time to analyse in this simulation which is the wavefront of impulse voltage (0.6 µs-1.2 µs) and wave tail of impulse voltage (1.2 µs-60 µs).

Result and Discussion

In this study, the result analyses are based on the time of impulse voltage, which is 0 s to 60 µs, and the result will focus on the impulse voltage's rising time and fall time. Also, we can see the effect of the electric field when the rising time impulse voltage is 0.6 µs - 1.2 µs and the fall time is 1.2 µs - 60 µs Fig. 6.
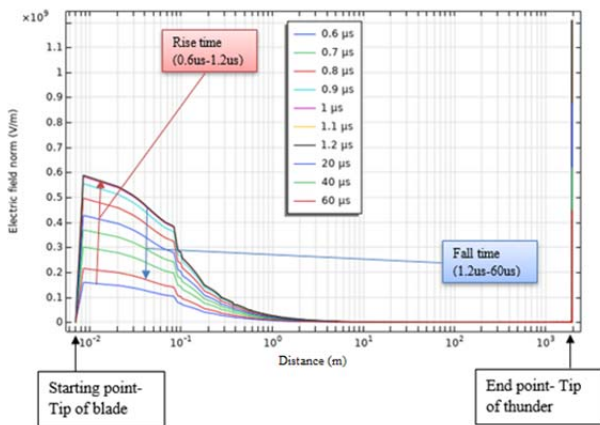
Fig. 5. 1D Plot graph electric field norm vs arc length

The result we recorded from finite element analysis shows the lightning phenomenon whereas the maximum electric field changes depending on the type of gas in the air.

Fig. 6 shows the strength of the electric field on the wind turbine blade under (Air), and various gases mixed.

Air gas (N) only

Fig. 7 shows the relationship of electric field versus distance with the simulation of lightning with air N_2. the point of cutline is defined from the blade tip to the bottom end of the thunder cloud.

In Fig. 7, the wind turbine blade and simulation results are influenced by electrical field distribution under Nitrogen, which accounts for most of the atmosphere. The maximum electrical field is 1330 MV/m at the thundercloud tip Fig. 6. Hence the record of the electrical field at the blade tip is 281-450 MV/m. Under the

Various Gases

Fig. 6 shows the graph of electric field norm versus time with various gas. This graph data was taken from Table 2. From this simulation result we recorded, the simulation under air and N_2 shows the exact value of the electric field norm. After combining N_2 and O_2, the electric field norm is lower than N_2. From the graph below, SO_2 contribute the highest maximum electric field norm, 1700 MV/m.
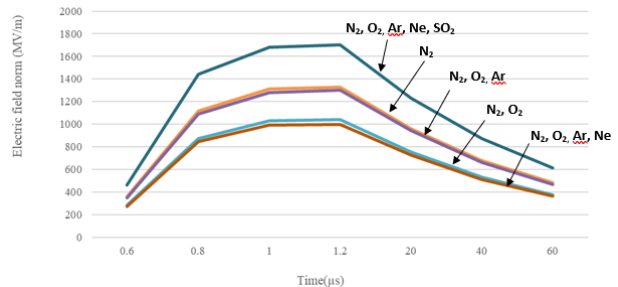
Fig. 6. Plot graph of electric field norm vs time with various gas

Fig. 8 shows the strength of the electric field norm versus arc length under various gas. The combination type of gas for this result is O_2, N_2, Ar, Ne and SO_2.

The maximum value of the electric field norm at the tip of a thunder cloud is 1700 MV/m which is the peak of an electric field value. Meanwhile, the electrical field norm at the blade tip is around 550 – 600 MV/m at 1.2 µs.
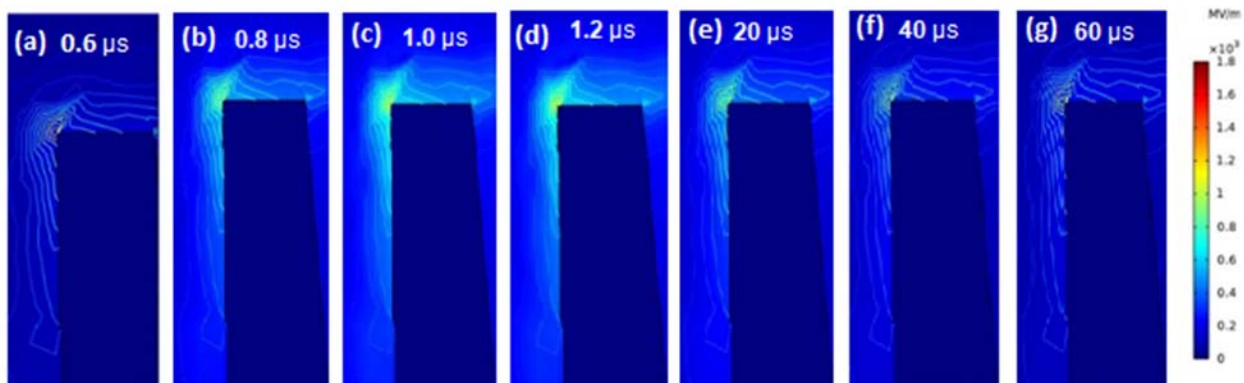
Fig. 7. Simulation result under Air-gas (N_2) showing e-field changes at the tip of the blade
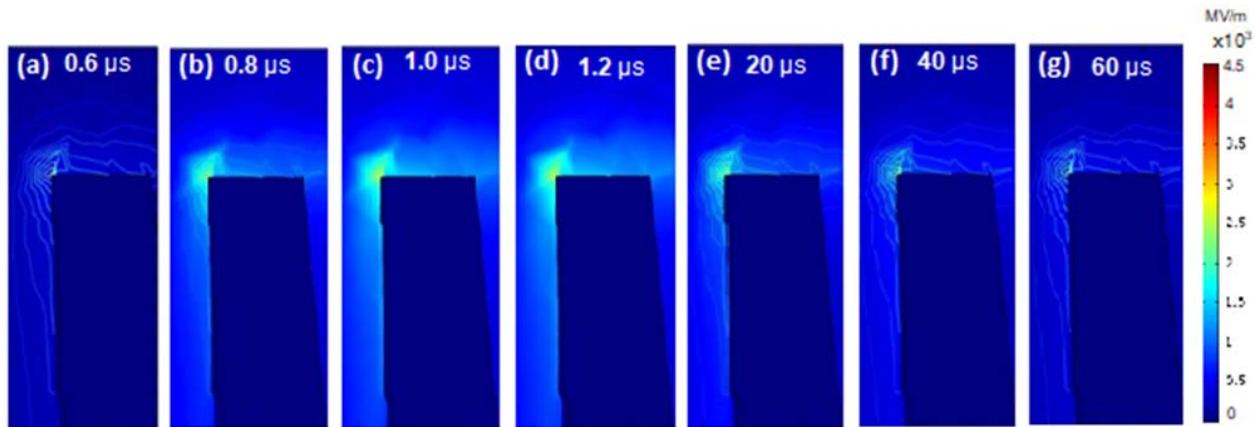
Fig. 8. Simulation result under gas O2, N2, Ar, Ne and SO₂ showing e-field changes at the blade's tip.

Table 2. Simulation results under various gas

Gas Type	Maximum of Electric Field Norm (MV/m)						
	Time(µs)						
	0.6	0.8	1.0	1.2	20	40	60
Nitrogen	359	1120	1310	1330	963	680	485
Nitrogen & Oxygen	281	874	1030	1040	755	531	376
Nitrogen, oxygen & argon	351	1090	1280	1300	944	664	470
Nitrogen, oxygen, argon & neon	272	845	992	1000	728	513	363
Nitrogen, oxygen, argon, neon & sulfur dioxide	461	1440	1680	1700	1230	873	615

Conclusion

We have modelled the formation of downward streamers transition under O₂, N₂, Ar, Ne and SO₂ gases. In all modelling, we analyse the wind turbine environment in finite element analysis in a time-dependent study to investigate the electric field distribution of wind turbine blades under impulse voltage with various gases.

For impulse wave generation, use three stages impulse generator. Switches are used to approximate the stage sphere gaps.

The results were analysed based on the time of impulse voltage from 0 – 60 µs. Moreover, the effect of the electrical field when the rising time impulse voltage is 0.6 µs-1.2 µs and the fall time is 1.2 µs-60 µs.

From the discussed result, the effect of air and N₂ shows the exact value of the electric field norm because these gases might have the same composition and not mix with other gases.

The effect of Air (N₂) gas, when applied to the entire domain, recorded the value of 1330 MV/m at the cloud tip, and on the other side, the electrical field strength on the blade varied from 281-450 MV/m within the raising time 0.6 µs - 1.2 µs.

Appling various gases to the modelling domain can change the electric field strength at the blade and thundercloud. From all mixtures of gases used in this modelling, the presence of SO₂ in the gas mixture can significantly affect electrical field strength. For example, it is clear to see when O2, N2, Ar and Ne are applied to the domain; the electrical field reading shows 1000 MV/m. However, when we add SO₂ to the same mixture, it hits 1700 MV/m.

REFERENCES
[1] O. Apata and D. T. O. Oyedokun, "An overview of control techniques for wind turbine systems," *Sci. African*, vol. 10, p. e00566, 2020, doi: 10.1016/j.sciaf.2020.e00566.

[2] R. D. Goud, R. Rayudu, C. P. Moore, and T. Auditorey, "An Evaluation of Potential Rise in a Wind Turbine Generator Earthing System During a Direct Lightning Strike," *Proc. Conf. Ind. Commer. Use Energy, ICUE*, vol. 2018-Octob, no. October, 2019, doi: 10.23919/ICUE-GESD.2018.8635648.

[3] T. Chady *et al.*, "Wind turbine blades inspection techniques," *Prz. Elektrotechniczny*, vol. 92, no. 5, pp. 3–6, 2016, doi: 10.15199/48.2016.05.01.

[4] A. Andreotti, G. Lupò, and C. Petrarca, "Evaluation of EM fields from return stroke for indirect - Lightning protection of wind turbines," *4th Int. Conf. Clean Electr. Power Renew. Energy Resour. Impact, ICCEP 2013*, no. January 2016, pp. 755–759, 2013, doi: 10.1109/ICCEP.2013.6586942.

[5] Z. A. Baharudin, N. A. Ahmad, J. S. Mäkelä, M. Fernando, and V. Cooray, "Negative cloud-to-ground lightning flashes in Malaysia," *J. Atmos. Solar-Terrestrial Phys.*, vol. 108, pp. 61–67, 2014, doi: 10.1016/j.jastp.2013.12.001.

[6] E. Shulzhenko, M. Krapp, M. Rock, S. Thern, and J. Birkl, "Investigation of lightning parameters occurring on offshore wind farms," *2017 Int. Symp. Light. Prot. XIV SIPDA 2017*, no. October, pp. 169–175, 2017, doi: 10.1109/SIPDA.2017.8116919.

[7] J. Nie *et al.*, "Lightning risk assessment of wind turbines in mountainous areas," *7th IEEE Int. Conf. High Volt. Eng. Appl. ICHVE 2020 - Proc.*, pp. 2020–2023, 2020, doi: 10.1109/ICHVE49031.2020.9279548.

[8] G. Masłowski, R. Ziemba, and T. Kossowski, "Przepięcia w liniach napowietrznych wywołane pobliskim wyładowaniem atmosferycznym," *Prz. Elektrotechniczny*, vol. 94, no. 2, pp. 41–44, 2018, doi: 10.15199/48.2018.02.10.

[9] C. Köhn, O. Chanrion, M. B. Enghoff, and S. Dujko, "Streamer Discharges in the Atmosphere of Primordial Earth," *Geophys. Res. Lett.*, vol. 49, no. 5, pp. 1–11, 2022, doi: 10.1029/2021GL097504.

[10] J. Holboll, S. F. Madsen, M. Henriksen, K. Bertelsen, and H. V Erichsen, "Discharge Phenomena in The Tip Area of Wind Turbine Blades and Their Dependency on Material and Environmental Parameters," *Light. Prot. (ICLP), 2006 Int. Conf.*, no. April, pp. 1503–1508, 2006.

[11] Z. Liu, H. Zhang, X. Hao, H. Jin, and K. Chen, "Research on Electric Field Distribution of Multiple wind turbines under Lightning Conditions," *7th IEEE Int. Conf. High Volt. Eng. Appl. ICHVE 2020 - Proc.*, pp. 2020–2023, 2020, doi: 10.1109/ICHVE49031.2020.9280000.

[12] I. D. Carmein, A. Arbor, M. I. Us, D. White, A. Arbor, and M. I. Us, *(12) United States Patent (10) Patent No .:*, vol. 2, no.

12. doi: 10.1109/FPS-2005.204208.

[13] S. L. J. Millen and A. Murphy, "Modelling and analysis of simulated lightning strike tests: A review," *Compos. Struct.*, vol. 274, no. July, p. 114347, 2021, doi: 10.1016/j.compstruct.2021.114347.

[14] A. Chusov, E. Rodikova, and D. Belko, "Simulation of an Impulse Arc Discharge in Line Lightning Protection Devices," p. 2, 2017.

[15] T. Feng, W. He, and J. G. Wang, "FEM Simulation of Charge Accumulation Behaviours on Polyimide Surface in 10 kV Negative High-Voltage Corona Polarization Process," *IEEE Access*, vol. 8, pp. 113151–113162, 2020, doi: 10.1109/ACCESS.2020.3003655.

[16] A. A. Eddib and D. D. L. Chung, "Electric permittivity of carbon fiber," *Carbon N. Y.*, vol. 143, pp. 475–480, 2019, doi: 10.1016/j.carbon.2018.11.028.

[17] L. Mishnaevsky, K. Branner, H. N. Petersen, J. Beauson, M. McGugan, and B. F. Sørensen, "Materials for wind turbine blades: An overview," *Materials (Basel).*, vol. 10, no. 11, pp. 1–24, 2017, doi: 10.3390/ma10111285.

[18] W. J. Jenkins, D. E. Lott, and K. L. Cahill, "A determination of atmospheric helium, neon, argon, krypton, and xenon solubility concentrations in water and seawater," *Mar. Chem.*, vol. 211, no. February, pp. 94–107, 2019, doi: 10.1016/j.marchem.2019.03.007.

[19] P. Orellano, J. Reynoso, and N. Quaranta, "Short-term exposure to sulphur dioxide (SO2) and all-cause and respiratory mortality: A systematic review and meta-analysis," *Environ. Int.*, vol. 150, p. 106434, 2021, doi: 10.1016/j.envint.2021.106434.